1 **Effect of enhancers and inhibitors on photocatalytic sunlight**

2 **treatment of dye wastewater**

3

4

5 Wennie Subramonian, Ta Yeong Wu*

6

7 Chemical Engineering Discipline, School of Engineering, Monash University, Jalan Lagoon

8 Selatan, Bandar Sunway, 46150, Selangor Darul Ehsan, Malaysia.

9

10 *Corresponding author: Ta Yeong Wu

11 **E-mail addresses**: _wu.ta.yeong@monash.edu_; _tayeong@hotmail.com_

12 **Tel**: +60 3 55146258

13 **Fax**: +60 3 55146207

14

15

16

17

18 **Abstract**

19 In view of the fatal illnesses which Methylene Blue (MB) leads to upon ingestion, the present

20 study focused on the use of natural sunlight in heterogeneous photocatalysis to decolourize

21 MB. Most past studies utilized UV, visible or simulated sunlight in photocatalysis of MB. The

22 present study also investigated the effects of enhancers (hydrogen peroxide and persulphate

23 ion) and inhibitors (chloride and carbonate ions) on photodecolourization of MB. Pseudo-first-

24 order rate constants for each studied effect were determined through Langmuir-Hinshelwood

25 model. The recommended conditions to photodecolourize 60 ppm of MB under natural

26 sunlight were 1.0 g/L titanium dioxide nanopowder at initial pH 10.5 in order to achieve

27 85.3% decolourization (rate constant of 10.8×10^{-3} min^{-1}). The addition of 4080 ppm hydrogen

28 peroxide and persulphate ion significantly enhanced the decolourization efficiency up to 96.6

29 and 99.3%, respectively (rate constants of 66.2 and 91.0×10^{-3} min^{-1}, respectively). However,

30 the addition of 2000 ppm chloride and carbonate ions reduced the decolourization efficiency

31 of MB to 74.7 and 70.2%, respectively (rate constants of 7.8 and 7.3×10^{-3} min^{-1}, respectively).

32 The present study implied that it was possible to use natural sunlight as a light source for

33 photocatalytic treatment of dye in tropical countries like Malaysia.

34

36

37 **Introduction**

38 One of the major pollutants found in water resources discharged around industrial areas is dye

39 and more than one million ton of dyes are produced annually worldwide (Chiu et al., 2010).

40 Treatment of wastewater containing dyes is one of the growing needs of the present time

41 because most dyes with a complex aromatic molecular structure are considered to be non-

42 oxidizable substances by traditional biological and physical treatment (Kumar and Bansal,

43 2012; Sun et al., 2013). It is estimated that 90% of total dyes produced are used in fabrics

44 whereas the remaining in leather, paper, plastic and chemical industry (Pandg and Abdullah,

45 2013). In 2011, there were 662 licensed textile and clothing industries in Malaysia,

46 representing a total investment of USD 2.6 billion (Saheed, 2012). However, 15% of the total

47 world production of dyes is lost during the dyeing process and released in textile effluents

48 (Lachheb et al., 2002). In fact, World Bank estimates that 17-20% of industrial water pollution

49 comes from textile dyeing and treatment industries (Chan et al., 2011). The textile wastewater

50 treatment has been considered as one of the most important categories of water-pollution

51 control due to its high colour intensity and high organic contamination (Lee et al., 1999).

52 The chosen dye in this study was Methylene Blue (MB). MB is a cationic dye which is

53 extensively used in dyeing industry (Saif Ur Rehman and Han, 2013). Advanced Dyestuff and

54 Chemicals Pvt. Ltd. (2011) reported that MB is one of the major dyes imported into Malaysian

55 textile industry, printing industries and occasionally in the medical field. A toxicology test

56 among 7 adult men and found that 26% MB was absorbed by the body from the consumption

57 of a 10 mg MB gelatin capsule (National Toxicology Program, 2013). It was also concluded

58 that acute ingestion of MB led to increasing heart rate, cyanosis, shock, vomiting,

59 quadriplegia, Heinz body formation and tissue necrosis in humans (National Toxicology

60   Program, 2013). Lodha et al. (2010) further stated that overdose of MB caused nausea,

61   abdominal and precardial pain, dizziness, headache, profuse swelling, sweating and mental

62   confusion.

63   Conventional dye wastewater treatment methods include physicochemical and biological

64   methods (Álvarez et al., 2013; Wang et al., 2014). According to Wang et al. (2014), these

65   conventional treatment methods for dye wastewater are proven unsatisfactory. Biological

66   methods result in lower decolourization efficiency due to inconsistency in quality and quantity

67   of wastewater discharged (Lee et al., 1999). Also, the use of biological treatment system alone

68   results in the incomplete degradation of recalcitrant compounds (Ghaly et al., 2011).   In

69   addition, degradation of dyes under anaerobic conditions produces aromatic amines, which are

70   carcinogenic and more hazardous (Low et al., 2012). Membrane separation suffers from

71   membrane fouling and higher in cost due to regular change of membrane. Chemical methods

72   are still widely favoured and used due to high degradation ability and generation of powerful

73   oxidizing agents but the efficiencies are strongly influenced by the type of oxidant (Forgacs et

74   al., 2004; Kitture et al., 2010).

75   Recently, degradation of dyes through oxidative methods receives considerable attention

76   because of its ability to degrade coloured aromatic compounds effectively (Vujevic et al.,

77   2010). The main mechanism of Advanced Oxidation Processes, AOPs is the generation of

78   highly reactive hydroxyl radicals, OH· (Gümüş and Akbal, 2011). OH· radicals are

79   electrophiles that react with most electron-rich organic compounds such as dyes to decompose

80   them into less harmful compounds such as carbon dioxide and water (Chan et al., 2011). There

81   are several methods of AOP that are currently in practice to treat dye wastewater such as

82 Fenton oxidation, ultrasonic cavitation and photochemical oxidation. Fenton oxidation

83 involves the production of reactive OH· under acidic condition through catalytic

84 decomposition of hydrogen peroxide (Güçlü et al., 2013). However, complexity of Fe(III)

85 hydrolysis and its high impact on reaction rates require additional care to obtain well-defined

86 iron salt solutions (Sievers, 2011). On the other hand, ultrasonic cavitation arises from

87 acoustic cavitation, namely the formation, growth and implosive collapse of bubbles in

88 liquids, which generates OH· for chemical reactions (Wu et al., 2013). Ultrasonic cavitation

89 usually incurs higher capital and maintenance cost as compared to ozone or UV treatment due

90 to the energy loss in the ultrasonic system (Chowdhury and Viraraghavan, 2009).

91 Photochemical oxidation was chosen in this study because of its high efficiency in

92 mineralization of organic compounds and feasibility with sunlight (Ong et al., 2012). Titanium

93 (IV) dioxide or TiO_2 was chosen as a photocatalyst for its non-toxicity, high photostability,

94 chemical inertness and resistivity against chemical corrosion (Kavitha and Palanisamy, 2010;

95 Tabaei et al., 2012). In addition, TiO_2 has higher photoreactivity due to its slower electron-

96 hole recombination as compared to zinc oxide, Hombikat, cadmium sulphide, zinc sulphide

97 and iron (III) oxide. Due to relatively low specific surface area of standard TiO_2 powder, TiO_2

98 nanopowder was used in order to provide more active sites (Low et al., 2012).

99   The reaction pathway of MB degradation through generation of radicals from

100 photogenerated electron-hole pairs (e_{CB}^-, h_{VB}^+) is shown as follow:

101    $TiO_2 + MB \leftrightarrow TiO_2\text{-}MB$ (1)

102    $TiO_2\text{-}MB + hv \leftrightarrow (e_{CB}^-, h_{VB}^+)\text{-}MB$ (2)

103    $h_{VB}^+ + H_2O \rightarrow OH\cdot + H^+$ (3)

104 $h_{VB}^+ + OH^- \rightarrow OH\cdot$ (4)

105 $e_{CB}^- + O_2 \rightarrow O_2^-\cdot$ (5)

106 $OH\cdot + MB \rightarrow$ intermediate products $\rightarrow$ degradation products (6)

107 $O_2^-\cdot + MB \rightarrow$ intermediate products $\rightarrow$ degradation products (7)

108 Eq. (1): Adsorption-desorption equilibrium is achieved between TiO_2 catalyst surface and MB

109 during stirring process in the dark.

110 Eq. (2): TiO_2-MB suspension is exposed to sunlight. TiO_2 has band gap energy of 3.2 eV (Zhou

111 et al., 2012). Only light energy with photons greater than the band gap energy is able to excite

112 electrons from the valence band to the conductive band of TiO_2 (Song and Bai, 2010).

113 Therefore, e_{CB}^- and h_{VB}^+ are generated.

114 Eqs. (3)-(4): Photogenerated holes in the valence band react with adsorbed water molecules

115 and hydroxide ions on the catalyst surface to form hydroxyl radical (Wu and Chern, 2006;

116 Gümüş and Akbal, 2011).

117 Eq. (5): The photogenerated electrons in the conduction band are scavenged and react with

118 oxygen molecules that are adsorbed on the catalyst surface to form superoxide radical ions

119 (Wu and Chern, 2006).

120 Eqs. (6)-(7): The generated hydroxyl radicals and superoxide anion radicals from Eqs. (3)-(4)

121 react with MB and degrade it into less harmful products such as carbon dioxide, nitrate,

122 ammonium and sulphate ions (Houas et al., 2001).

123 Although previous studies investigated the degradation of synthetic dye wastewater using

124 photocatalysis, most of the past studies focused on the use of pure or modified catalyst under

125 UV or visible light as a light source (Lee et al., 1999; Houas et al., 2001; Lachheb et al., 2002;

126   Li and Li, 2002; Chen et al., 2003; Lin et al., 2007; Su et al., 2012). In many countries, both

127   energy and waste management systems are under changes (Nouri et al., 2012). Thus, the

128   present study utilized natural sunlight and commercially available catalyst in photocatalytic

129   treatment of MB wastewater. In tropical countries like Malaysia, ample sunlight is available

130   throughout the year, leading to more favourable, sustainable and economical photocatalytic

131   process using sunlight as a light source (Pardeshi and Patil, 2009).

132   Textile industrial wastewater comprises of several chemical and organic compounds, such

133   as salts, detergents, organic acids, dyestuffs, dying aids, and sizing agents (Fu et al., 2011;

134   Lotito et al., 2012). The degradation of those organic substrates leads to the generation of ions,

135   such as chloride and carbonate ions, that may inhibit photocatalysis (Wang et al., 2000; Mota

136   et al., 2008). Past studies reported a decrease in photocatalytic activity of up to 20-30% in the

137   presence of Cl^- and CO_3^{2-} (Lee et al., 1999; Zhou et al., 2010).Therefore, it is crucial to

138   investigate the effect of inhibitors (Cl^- and CO_3^{2-}) on the photocatalytic degradation of MB.

139   On the other hand, the roles of enhancers, namely hydrogen peroxide (H_2O_2) and

140   persulphate ions ($S_2O_8^{2-}$), in photocatalysis of MB were also studied to determine their

141   significance during photodegradation. H_2O_2 was reported as an oxidant that enhanced photo-

142   oxidation treatment in small quantity (Boroski et al., 2008). The use of persulphate ions,

143    $S_2O_8^{2-}$ have attracted increasing attention due to their greater oxidizing potential (1.82-2.02 V)

144   as compared to H_2O_2 (1.76 V) (Chen et al., 2012). For examples, H_2O_2 and $S_2O_8^{2-}$ enabled

145   two-fold increases in decolorization of Maxilon Navy dye and methyl orange, respectively

146   (Ghaly et al., 2007; Anandan, 2008). Thus, the effect of enhancers (H_2O_2 and $S_2O_8^{2-}$) on the

147   photocatalytic degradation of MB was also investigated in this study.

148 To the best of our knowledge, no significant studies were previously conducted on

149 utilizing sunlight and unmodified TiO_2 for photocatalytic treatment of MB under the influence

150 of enhancers or inhibitors which were found in dye industries. Thus, the main goal of the

151 present study was to investigate the recommended conditions and effects of various operating

152 parameters such as (a) initial concentration of MB; (b) initial pH of solution; (c) catalyst

153 dosage; (d) hydrogen peroxide, persulphate ions, chloride ions and carbonate ions on the

154 decolourization efficiency of MB. The kinetic model on decolourization of MB using natural

155 sunlight in Malaysia was also investigated.

156

157 **2 Materials and Methods**

158 2.1 Materials

159 MB dye with 98.7% purity, (molecular weight of 319.85g/mol and λ_{max} at 664nm) was

160 purchased from Sigma-Aldrich (USA) and it was used without further purification. The

161 molecular structure of MB is illustrated in Fig. 1. TiO_2 nanopowder with 99.7% purity was

162 purchased from Sigma-Aldrich (USA) and used as photocatalyst without further modification.

163 The TiO_2 nanopowder has particle size of < 25 nm and a specific surface area of 200-220

164 m^2/g. The initial pH value of the MB dye solution was adjusted by using 1 mol/L HCL or 1

165 mol/L NaOH solution.

166

167 2.2 Photoreactor and sunlight illumination

168 The photoreactor was 17 cm × 11 cm × 5 cm (Length x Width x Depth) in dimension with

169 volume capacity of 650 ml. The photoreactor was set up on a magnetic stirrer at an open space

170 under maximum sunlight exposure. Sunlight intensity was measured using a WalkLAB Digital

171 Lux meter (Trans Instruments (S) Pte. Ltd., Singapore).

172   2.3 Experimental procedures

173   MB solution of 500 ml was prepared at desired initial concentration (30-70 ppm), initial pH

174   value (7.5-13.5) and catalyst loading (0.5-2.5 g/L). The concentration range chosen in the

175   present study based on the discharge concentration of a dye plant in Malaysia. The

176   concentration range was chosen in the present study based on approximately the discharge

177   concentration of a dye plant in Malaysia. Furthermore, the presence of a very small amount of

178   dye in water (<1 mg/L for some dyes) is highly visible and enough to present an aesthetic

179   problem (Low et al., 2012). The solution was stirred in the dark for 30 minutes to achieve

180   adsorption-desorption equilibrium. The suspension was then continuously stirred under

181   sunlight from 11 am to 3 pm, during which, the natural sunlight in Malaysia had stable

182   illuminance in the range of 80 to 110 klux. Therefore, all experimental runs were conducted

183   during the aforementioned time frame. The treated MB was sampled every 30 minutes and

184   was centrifuged at 14000 rpm for 15 minutes using Profuge 14k Centrifuge to separate the

185   TiO_2 catalyst. Then, the decolourization efficiency was observed by measuring the absorbance

186   of the supernatant using GENESYS 10UV spectrophotometer (Thermo Fisher Scientific Inc,

187   USA) at a wavelength of 664 nm. The decolourization efficiency was determined by:

188   Decolourization efficiency (%) = $(C_o - C_{f,t}) / C_o \times 100\%$ (8)

189   where C_o is the initial dye concentration (mg/l) and $C_{f,t}$ is the final concentration (mg/l) after

190   photodecolourization at time t. Experiments were conducted at surrounding temperature and

191   repeated three times to demonstrate the reproducibility of results. The effects of hydrogen

192   peroxide (510-4080 ppm), persulphate ions (510-4080 ppm), chloride ions (500-2000 ppm)

193   and carbonate ions (500-2000 ppm) were evaluated subsequently using the predetermined

194 recommended conditions of initial concentration of MB, catalyst loading and initial pH. All

195 enhancers and inhibitors were prepared as stock solutions and added into the photocatalytic

196 system following the desired concentration. Control experimental runs were carried out as

197 tabulated in Table 1. Finally, kinetic analysis was performed on all effects.

198 **3 Results and discussion**

199 3.1 Effect of initial concentration

200 Generally, composition of MB in dye wastewater may vary. Hence, it is of interest to study the

201 influence of intial concentration of MB on the decolourization efficiency. Controls A and B

202 (Figs. 2-4) proved that decolourization of MB was not feasible in the absence of natural

203 sunlight and photocatalyst. On the other hand, the use of natural sunlight and photocatalyst

204 resulted in significant MB decolourization efficiency (Figs. 2-8). Fig. 2 shows that when the

205 initial concentration of MB increased from 30 to 70 ppm, the decolourization efficiency of

206 MB decreased. The increase in MB concentration resulted in an increase of MB molecules.

207 Hence, light penetration into the solution was reduced (Akbal, 2005), decreasing the path

208 length of photons entering the solution (Muruganandham et al., 2007). The number of active

209 sites to generate hydroxyl radicals decreased due to the fewer photons reaching the catalyst

210 surface. Therefore, photocatalytic activity decreased with increasing initial concentration of

211 MB.

212 Fig. 2 shows that there was still a very minimal decolourization of 5.5% in the dark for

213 control A. This was due to the adsorption of some MB molecules on TiO_2 catalyst surface

214 (Kansal et al., 2007). Therefore, minimal decolourization was observed albeit in the absence

215 of sunlight. Decolourization of 13.0% was also observed in the absence of TiO_2 for control B

216 (Fig. 2). This was due to the excitation of MB molecules when they were irradiated under

217   sunlight which led to direct degradation of MB (Hashim et al., 2001). However, the

218   decolourization in the absence of catalyst (control B) was ineffective as compared to the

219   presence of catalyst. Generally, an increase in initial dye concentration reduces the

220   decolourization efficiency (Neppolian et al., 2002). However, the present study showed no

221   significant difference in maximum decolourization of MB between the initial concentrations

222   of MB from 30 to 60 ppm after 4 hours of photodecolourization (Fig. 2). In addition, 60 ppm

223   was the highest initial concentration to achieve at least 80% of maximum decolourization.

224   Therefore, an initial concentration of 60 ppm would be used for the subsequent investigations.

225   Literature reviews suggested that heterogeneous photocatalysis follows the Langmuir-

226   Hinshelwood, L-H kinetic expression as shown in Eq. (8). It is deemed the most appropriate

227   model to describe a plateau-type kinetic profile (Figs. 2-8) in which the rate of decolourization

228   increases with photodecolourization time until the rate becomes zero (Yang et al., 2005;

229   Pouretedal and Kadkhodaie, 2010).

230
$$r = -\frac{dC}{dt} = \frac{kK_{dye}C}{1 + K_{dye}C_{initial}} \qquad (9)$$

231   Eq. (9): $C_{initial}$ is the initial concentration of MB (ppm or mg/L). K_{dye} is the L-H adsorption

232   equilibrium constant, (L/mg) and it represents the catalyst adsorption capacity. k is the rate

233   constant of the surface reaction (mg/L.min) and it is the proportionality constant for the

234   intrinsic reactivity of photo-activated surface with C.

235   At low initial concentration of MB (< 300 ppm), Eq. (9) can be simplified into a pseudo-

236   first-order equation as shown in Eq. (10) (Nezamzadeh-Ejhieh and Hushmandrad, 2010).

237
$$r = -\frac{dC}{dt} = k_{app}C \qquad (10)$$

238   Eq. (9): k_{app} (min^{-1}) is the pseudo-first-order rate constant and it serves as a comparison and

239   description for the photocatalytic reaction rate in the reactor system (Low et al., 2012).

240   Further integration and rearranging of Eqs. (10), (11) and (12) are obtained (Low et al.,

241   2012). Straight line plots of ln C against time yielded k_{app} values for different effects (Table 2-

242   3). k_{app} values were used for the kinetic study of this research.

243                                   $$C = C_0 e^{-k_{app}t}$$ (11)

244                                   $$\ln C = -k_{app}t + \ln C_0$$ (12)

245

246   k_{app} for 70 ppm was 54% lower than 30 ppm (Table 2). Reduction in k_{app} values at higher

247   initial concentration of MB (Table 2) further proved that the increase in initial concentration of

248   dye led to a decrease in photocatalytic activity.

249

250   3.2 Effect of catalyst loading

251   In order to reduce the economical cost of using large quantity of catalyst, it is of great desire to

252   achieve high decolourization efficiency with minimal usage of catalyst loading during

253   wastewater treatment process. Therefore, the recommended catalyst loading for effective MB

254   decolourization was investigated in the present study. Fig. 3 and Table 2 show that at lower

255   TiO$_2$ loading, lower percentage of decolourization and k_{app} values were observed due to the

256   lacking of catalyst (such as 0.5 g/L of catalyst loading) to fully utilize the transmitted light to

257   form active sites (Kavitha and Palanisamy, 2010). As the catalyst dosage gradually increased

258   from 0.5 to 1.5 g/L, more catalyst was present in the solution to be activated by photons,

259   hence, more active sites were generated, which in return generated more hydroxyl radicals

260   (Lee et al., 1999). Thus, the number of MB molecules adsorbed on active sites and

261   decolourized by hydroxyl radicals increased. Therefore, photocatalytic activity accelerated

262   when catalyst loading increased gradually. An increase of k_{app} values from 0.5 to 1.5 g/L of

263   catalyst dosage is shown in Table 2.

264   However, Fig. 3 also shows that the decolourization of MB decreased when the catalyst

265   loading was further increased above 1.5 g/L (2.0 to 2.5 g/L). This phenomenon was attributed

266   to an excessive amount of TiO_2 present in the solution that contributed towards higher

267   suspension turbidity in the solution (Lee et al., 1999). Thus, light scattering increased due to

268   the presence of excessive catalyst which reduced light penetration (Franco et al., 2009;

269   Herney-Ramirez et al., 2010). Fewer photons reached and activated the catalyst surface,

270   leading to the reductions of active sites and fewer generations of hydroxyl radicals (Franco et

271   al., 2009). In short, further addition of catalyst dosage beyond a specific limit did not enhance

272   the photocatalytic activity but deteriorated it. Similar phenomenon was observed by Xiao et al.

273   (2008), who found that an increase of catalyst loading from 0.5 to 1.0 g/L enhanced the

274   decolourization of MB but a decline in efficiency was observed when higher dosage of

275   catalyst was used (> 1.0 g/L). Based on Fig. 3 and Table 2, catalyst loading of 1.5 g/L

276   achieved the highest decolourization efficiency and pseudo-first-order rate constant. However,

277   the difference in maximum decolourization efficiency between 1.0 and 1.5 g/L was

278   insignificant whereby the former and later achieved 85.8 and 91.7%, respectively. Apart from

279   that, smaller catalyst dosage is less economical costing for industrial practices as compared to

280   the use of higher catalyst dosage with similar decolourization efficiency outcome. Therefore,

281   catalyst loading of 1.0 g/L was the chosen catalyst dosage for the subsequent investigations.

282
283

284   3.3 Effect of initial pH

285   In general, dye wastewater discharged from industries has a wide range of pH values. Since

286   the generation of hydroxyl radicals is affected by pH conditions, the variation of pH should be

287   taken into account in the treatment of dye wastewater. Study on the influence of initial pH

288   showed that the decolourization of MB and pseudo-first-order rate constants increased with

289   increasing pH from 7.5 to 13.5 as shown in Fig. 4 and Table 2. MB dissolved as a cationic dye

290   in aqueous solution. The surface charge of TiO_2 catalyst became more negative as the pH of

291   the solution increased. Hence, a stronger adsorption was formed between the positively

292   charged MB cations and negatively charged TiO_2 surface due to electrostatic interaction

293   (Senthilkumaar et al., 2006). Therefore, a higher rate of decolourization was achieved at

294   higher pH values.

295   An increase of k_{app} values could be observed when the treatment process was conducted in

296   more alkaline condition (Table 2). Based on Fig. 4, the lowest initial pH to achieve at least

297   80% maximum decolourization efficiency was pH 10.5. Although initial pH 12 and 13.5

298   exhibited higher maximum decolourization efficiency (Fig. 4) and at a faster rate (Table 2) as

299   compared to 10.5, the selection of high pH is not favorable in wastewater treatment. The

300   treated wastewater with higher initial pH value may impose a detrimental effect on any

301   downstream biological treatment process, especially to methanogenic bacteria during

302   anaerobic digestion (Appels et al., 2008). In addition, the increasing use of alkaline chemicals

303   is not environmentally sustainable and economically sound. Therefore, initial pH 10.5 was

304   selected for the subsequent investigations instead of initial pH 12 or 13.5.

305

306

307

308   3.4 Influence of enhancers

309   The use of enhancers (H_2O_2 and $S_2O_8^{2-}$) in the absence of sunlight and TiO_2 as a photocatalyst

310   (controls C-F) resulted in insignificant decolourization efficiency of MB. On the other hand,

311   H_2O_2 and $S_2O_8^{2-}$ experimental runs that were conducted under sunlight together with TiO_2

312   resulted in higher decolourization efficiency (Figs. 5-6). The results showed that higher

313   decolourization efficiency using H_2O_2 and $S_2O_8^{2-}$ could only be attained under sunlight and in

314   the presence of TiO_2. Subsequent investigations on the use of H_2O_2 and $S_2O_8^{2-}$ were performed
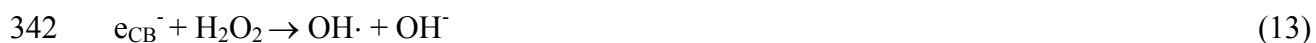
315   under sunlight and in the presence of TiO_2.

316

317   3.4.1 Hydrogen peroxide, H_2O_2

318   Rate of decolourization of dye wastewater can be significantly improved due to the presence

319   or addition of certain substances such as hydrogen peroxide (H_2O_2) (Giri et al., 2011). In order

320   to treat large capacity of dye wastewater, certain treatment plants choose to add photo-

321   assisting chemicals to degrade non-biodegradable pollutants more effectively (Lee et al.,

322   2011). Hence, this study investigated the influence of H_2O_2 on the decolourization of MB.

323   Results from Fig. 5 shows that the control O (without additive) achieved lower decolourization

324   efficiency as compared to experiments with H_2O_2 addition. According to Table 3, there was a

325   significant increase of 513% in k_{app} values between the absence of H_2O_2 and 4080 ppm of

326   H_2O_2. As the concentration of H_2O_2 added into the solution increased, the decolourization

327   efficiency (Fig. 5) and pseudo-first-order rate constants (Table 2) increased. H_2O_2 has electron

328   scavenging properties. Hence, H_2O_2 reacted with electrons from the conduction band of TiO_2

329   to form hydroxyl radicals (Mohapatra and Parida., 2006). An increase in concentration of

330   H_2O_2 led to an increase number of hydroxyl radicals generation, hence, more MB molecules

331   would be degraded by hydroxyl radicals. Therefore, decolourization efficiency increased with

332   an increase of H_2O_2. Although in the absence of catalyst, a significant decolourization of

333   35.5% was observed for control D (Fig. 5). This phenomenon was attributed to the direct

334   breakdown of H_2O_2 under sunlight to form hydroxyl radicals (Kavitha and Palanisamy, 2010).

335   For control C, slight decolourization of 14.3% was observed. This was due to adsorption

336   of MB molecules on catalyst surface. Thus, slight decolourization occurred although in the

337   absence of sunlight. By comparing the decolourization results obtained for control C against

338   510-4080 ppm of H_2O_2 under sunlight (Fig. 5), the influence of H_2O_2 was much significant

339   under sunlight because sunlight was able to accelerate the generation of active sites and direct

340   breakdown of H_2O_2 (Kavitha and Palanisamy, 2010). Hydroxyl radical was formed based on

341   the three reaction pathways as shown below (Kavitha and Palanisamy, 2010):

342    $e_{CB}^- + H_2O_2 \rightarrow OH\cdot + OH^-$ (13)

343    $H_2O_2 + O_2^-\cdot \rightarrow OH\cdot + H^+ + O_2$ (14)

344    $H_2O_2 + hv \rightarrow 2\ OH\cdot$ (15)

345   Eq. (13): When active sites are formed from TiO_2 under sunlight, H_2O_2 traps photogenerated

346   electrons from the conduction band of TiO_2 to generate hydroxyl radicals, inhibiting electron-

347   hole recombination.

348   Eq. (14): H_2O_2 reacts with superoxide anion generated from Eq. (5) to form hydroxyl radicals.

349   Eq. (15): H_2O_2 also converts directly into hydroxyl radicals under sunlight.

350

351   3.4.2 Persulphate ions, $S_2O_8^{2-}$

352   Fig. 6 shows that the decolourization efficiency obtained by 0 ppm $S_2O_8^{2-}$ was lower as

353   compared to the experiments with $S_2O_8^{2-}$ addition whereas there was an 743% increase in k_{app}

354   values between 0 ppm and 4080 ppm of $S_2O_8^{2-}$ (Table 3). The present result verified that the

355   addition of $S_2O_8^{2-}$ could significantly improve the decolourization efficieny of MB. $S_2O_8^{2-}$

356   showed a silmiar trend as H_2O_2, in which a gradual increase in $S_2O_8^{2-}$ resulted in significant

357   increase of MB decolourization because $S_2O_8^{2-}$ has electron scavenging properties (Das et al.,

358   2007). Hence, $S_2O_8^{2-}$ reacted with electrons from the conduction band of TiO_2 to form sulphate

359   radical anions. Sulphate radical anions would then react with water molecules to form

360   hydroxyl radicals. In short, an increase in concentration of $S_2O_8^{2-}$ led to an increase of both

361   sulphate radical anions and hydroxyl radicals. Therefore, decolourization efficiency increased

362   with increasing $S_2O_8^{2-}$.

363   Secondly, the generation of sulphate radical anions from $S_2O_8^{2-}$ also prevented electron-

364   hole recombination of TiO_2 (Kavitha and Palanisamy, 2010). When the concentration of $S_2O_8^{2-}$

365   increased, electrons in the conduction band of TiO_2 were continuously consumed by more

366   sulphate radical anions, resulting more valence band electrons would be promoted into the

367   conduction and leaving behind more photogenerated holes in the valence band. According to

368   Eqs. (3) and (4), more hydroxyl radicals could be generated in the presence of more

369   photogenerated holes. Therefore, decolourization efficiency was improved with an addition of

370    $S_2O_8^{2-}$. Thirdly, sulphate radical anions could react and degrade MB. Sulphate radical anions

371   also had a unique nature of attacking MB molecules in various positions which resulted in

372   fragmentation of MB molecules to occur rapidly (Neppolian et al., 2002). Therefore,

373   decolourization efficiency of MB increased when concentration of $S_2O_8^{2-}$ increased.

374   Control E and F (Fig. 6) had a higher maximum decolourization efficiecny as compared to

375   control C and D of H_2O_2 (Fig. 5). This phenomenon was due to strong oxidizing properties of

376    $S_2O_8^{2-}$ (Das et al., 2007). Sulphate radical anions formed from $S_2O_8^{2-}$ could react and degrade

377   MB molecules in the absence or presence of sunlight (Das et al., 2007). Therefore, $S_2O_8^{2-}$

378   addition in the dark was able to decolourize MB effectively. The following reaction pathways

379   summarize the photocatalytic activity of MB with an addition of $S_2O_8^{2-}$.

380    $S_2O_8^{2-} + e_{CB}^- \rightarrow SO_4^-\cdot + SO_4^{2-}$ (16)

381    $SO_4^- + H_2O \rightarrow OH\cdot + SO_4^{2-} + H^+$ (17)

382    $SO_4^-\cdot + e_{CB}^- \rightarrow SO_4^{2-}$ (18)

383    $SO_4^-\cdot + MB \rightarrow SO_4^{2-} + MB^+\cdot$ (intermediates) (19)

384    $SO_4^-\cdot + MB^+\cdot$ (intermediates) $\rightarrow SO_4^{2-} + CO_2 + HNO_3 +$ other inorganic (20)

385   Eq. (16): $S_2O_8^{2-}$ possesses electron scavenging properties and reacts with electrons from the

386   conduction band of TiO_2 to form sulphate radical anions (Kavitha and Palanisamy, 2010).

387   Eq. (17): Sulphate radical anions react with water molecules to generate hydroxyl radicals

388   (Das et al., 2007).

389   Eq. (18): Sulphate radical anions trap photogenerated electrons from the conduction band of

390   TiO_2 to prevent electron-hole recombination (Neppolian et al., 2002).

391   Eqs. (19)-(20): Sulphate radical anions are powerful oxidants that react and degrade MB

392   molecules (Das et al., 2007).

393

394

395

396   3.5 Influence of inhibitors

397   The use of inhibitors (Cl^- and CO_3^{2-}) in the absence of sunlight and TiO_2 as photocatalyst

398   (controls G-J) showed no improvement in decolourization efficiency of MB. Therefore,

399   subsequent investigations relating to the use of Cl^- and CO_3^{2-} were carried out under sunlight

400   and presence of TiO_2.

401

402   3.5.1 Chloride ions, Cl^-

403   Sodium chloride is found in dye wastewater as a result of sectional waste from textile mills

404   (Neppolian et al., 2002). Therefore, it is important to determine the treatment efficiency of

405   photocatalysis under the influence of Cl^-. Results obtained (Fig. 7 and Table 2) in this study

406   showed that the rate of decolourization decreased with increasing amount of Cl^-. Furthermore,

407   a decrease in k_{app} values from 10.8×10^{-3} (0 ppm of Cl^-) to 7.8×10^{-3} (2000 ppm of Cl^-)

408   indicated a decline in photocatalytic activity. A consumption of photogenerated holes by Cl^-

409   inhibited the generation of hydroxyl radicals (Eqs. 3 and 4), which in turn resulted in the

410   reduction of photocatalytic activity (Neppolian et al., 2002). Therefore, Cl^- exhibited strong

411   inhibiting effects for MB degradation, whereby an increase of Cl^- led to a decrease in

412   decolourization efficiency of MB.

413   Slight higher decolourization efficiency was observed for control G as compared to

414   control H (Fig. 7). This phenomenon was attributed to some of the MB molecules adsorbed on

415   the catalyst surface for control G. Therefore, percentage of decolourization for 2000 ppm Cl^-

416   in the dark was slightly higher than 2000 ppm under sunlight without catalyst. The inhibition

417 of OH· generation due to the consumption of photogenerated holes by Cl⁻ could be explained

418 by using two reaction pathways as shown below (Neppolian et al., 2002; Gaca et al., 2005):

419 $Cl^- + h_{VB}^+ \rightarrow Cl\cdot$ (21)

420 $Cl\cdot + Cl^- \rightarrow Cl_2^{\cdot-}$ (22)

421 Eq. (21): Cl⁻ reacts with photogenerated holes from valence band of TiO_2 to form chlorine

422 radicals.

423 Eq. (22): Chlorine radicals then react with Cl⁻ and convert into chloride radical anion.

424

425 3.5.2 Carbonate ions, CO_3^{2-}

426 Sodium carbonate is commonly used in textile processing operations to adjust the pH of the

427 dying bath (Neppolian et al., 2002). Hence, dye wastewater from textile industries may

428 contain traces of sodium carbonate. The present study also investigated the influence of CO_3^{2-}

429 on the decolourization efficiency of MB. Fig. 8 and Table 2 show that the percentage of

430 decolourization and k_{app} values decreased when the concentration of CO_3^{2-} increased. A

431 decrease in k_{app} values from 10.8 (0 ppm of CO_3^{2-}) to 7.3×10^{-3} min^{-1} (2000 ppm of CO_3^{2-})

432 further proved that the photocatalytic activity of MB declined with an increase of CO_3^{2-}. The

433 decrease in decolourization efficiency of MB was attributed to the hydroxyl radicals

434 scavenging properties of CO_3^{2-} (Lee et al., 1999). CO_3^{2-} reacted with hydroxyl radicals, hence,

435 reducing the number of hydroxyl radicals available. The decrease in hydroxyl radicals, which

436 served as a primary source for photodegradation of MB, reduced the decolourization

437 efficiency. Therefore, in photocatalytic process, CO_3^{2-} inhibited the degradation of MB. The

438 role of CO_3^{2-} could be explained by the following reaction pathway (Neppolian et al., 2002):

439    $CO_3^{2-} + OH\cdot \rightarrow CO_3^- + OH^-$ (23)

440   Eq. (23): CO_3^{2-} is consumed by reacting with hydroxyl radicals to generate carbonate radical

441   anion as oxidation transients.

442

443   3.6 Comparison of k_{app} values under the influence of enhancer and inhibitor

444   By comparing k_{app} values obtained for the experimental run without additives (Table 3), the

445   presence of H_2O_2 and $S_2O_8^{2-}$ increased the rate of photodecolourization by 38-513% and 36-

446   743%, respectively. On the other hand, an addition of Cl^- and CO_3^{2-} reduced the rate of

447   photodecolourization of MB by 15-28% and 13-32%, respectively. k_{app} values for both 2040

448   and 4080 ppm of $S_2O_8^{2-}$ were significantly higher as compared to the similar concentration of

449   H_2O_2 (Table 3). Thus, the results from the present study agreed with Poulios and Aetopoulou

450   (1999), that $S_2O_8^{2-}$ was a more powerful oxidizing agent in decolourizing MB as compared to

451   H_2O_2. However, the inhibitor strengths between Cl^- and CO_3^{2-} remained inconclusive due to

452   the similar k_{app} values obtained for both anions.

453   The value of k_{app} obtained from this study for different initial concentration of MB was

454   summarized and compared with the previous studies (Table 4). In general, higher values of

455   k_{app} were obtained in most of the past studies (Table 4). However, their results were mainly

456   attributed to the use of UV light source, lower concentration of MB and/or higher

457   concentration of TiO_2. The present study was performed comparatively good with k_{app} of 10.8

458    $\times 10^{-3}$ min^{-1} at 60 ppm MB and 1 g/L TiO_2 under sunlight up to 240 min. Under same

459   condition, the k_{app} was increased by 743% to 91.0 $\times 10^{-3}$ min^{-1} with an addition of 4080 ppm

460    $S_2O_8^{2-}$. Thus, this study indicated that higher concentration of MB could be treated under

461   tropical sunlight through photocatalytic process if certain amount of persulphate ions was

462   added into the treatment system. However, further investigations are needed to confirm the

463   effective use of persulphate ions under sunlight during the photocatalytic treatment of

464   wastewater, which consists of multiple dyes.

465

466   **4 Conclusions**

467   By studying the effects of initial concentration, initial pH and catalyst loading, it was found

468   that 85.2% of 60 ppm MB was successfully decolourized under 1.0 g/L of TiO_2 dosage and

469   initial pH 10.5. An increase of initial concentration but a decrease of pH would result in a

470   reduction of photocatalytic treatment of MB. The gradual increase of catalyst loading resulted

471   in the gradual increase of decolourization efficiency but further addition of catalyst after the

472   recommended catalyst dosage did not increase photocatalytic activity. An addition of strong

473   oxidizing agents such as H_2O_2 and $S_2O_8^{2-}$ further enhanced the photocatalytic activity of MB

474   up to 96.6% and 99.3%, respectively. In addition, persulphate ions concluded to be a stronger

475   oxidizing agent as compared to hydrogen peroxide. On the other hand, the presence of Cl^- and

476   CO_3^{2-} inhibited photocatalytic activity up to 74.7% and 70.2%, respectively.

477   In conclusions, this study proved that it is possible to achieve high decolourization

478   efficiency of dye using photocatalytic treatment under natural sunlight in a tropical country

479   like Malaysia, where an abundance of sunlight is made available throughout the year. It is an

480   economical and environmentally sustainable method to utilize sunlight as a natural source of

481   energy to treat dye wastewater through photocatalytic process.

482

483

487

488   **References**

489   Advanced Dyestuff and Chemicals Pvt. Ltd., 2011. Product List for Textile Applications.

490   http://www.textiledyes.net/textile-dyes.html. Accessed: 1 May 2011.

491   Akbal, F. (2005). Photocatalytic degradation of organic dyes in the presence of titanium oxide

492   under UV and solar light: effect of operational parameters. *Environmental Progress,*

493   *24*, 317-322.

494   Álvarez, M. S., Moscoso, F., Rodríguez, A., Sanromán, M. A., & Deive, F. J. (2013). Novel

495   physic-biological treatment for the remediation of textile dyes-containing industrial

496   effluents. *Bioresource Technology, 146*, 689-695.

497   Anandan, S. (2008). Photocatalytic effects of titania supported nanoporous MCM-41 on

498   degradation of Methyl Orange in the presence of electron acceptors. *Dyes and*

499   *Pigments, 76*, 535-541.

500   Appels, L., Baeyens, J., Degrève, J., & Dewil, R. (2008). Principles and potential of the

501   anaerobic digestion of waste-activated sludge. *Progress in Energy and Combustion*

502   *Science, 34*, 755-781.

503   Boroski, M., Rodrigues, A. C., Garcia, J. C., Gerola, A. P., Nozaki, J., & Hioka, N. (2008).

504   The effect of operational parameters on electrocoagiulation-flotation process followed

505   by photocatalysts applied to the decontamination of water effluents from cellulose and

506   paper factories. *Journal of Hazardous Materials, 160*, 135-141.

507   Chan, S. H. S., Wu, T. Y., Juan, J. C., & Teh, C. Y. (2011). Recent developments of metal

508   oxide semiconductors as photocatalysts in advanced oxidation processes (AOPs) for

509   treatment of dye wastewater. *Journal of Chemical Technology and Biotechnology, 86*,

510   1130-1158.

511   Chen, F., Zhao, J., & Hidaka, H. (2003). Adsorption factor of dye constituent aromatics on the

512   surface of TiO_2 in the presence of phosphate ions. *Research on Chemical*

513   *Intermediates, 29*, 733-748.

514   Chen, X., Wang, W., Xiao, H., Hong, C., Zhu, F., Yao, Y., & Xue, Z. (2012). Accelerated

515   TiO_2 photocatalytic degradation of Acid Orange 7 under visible light mediated by

516   peroxymonosulphate. *Chemical Engineering Journal, 193-194*, 290-295.

517   Chiu, W. S., Khiew, P. S., Cloke, M., Isa, D., Tan, T. K., Radiman, S., Abd-Shukor, R.,

518   Hamid, A. M. A., Huang, N. M., Lim, H. N., & Chia, C. H. (2010). Photocatalytic

519   study of two-dimensional ZnO nanopellets in the decomposition of Methylene

520   Blue. *Chemical Engineering Journal, 158***,** 345-352.

521   Chowdhury, P., & Viraraghavan, T. (2009). Sonochemical degradation of chlorinated organic

522   compounds, Phenolic Compounds and Organic Dyes –A Review. *Science of the Total*

523   *Environment, 407*, 2474-2492.

524   Das, D. P., Baliarsingh, N., & Parida, K. M. (2007). Photocatalytic decolorisation of

525   Methylene Blue (MB) over titania pillared zirconium phosphate (ZrP) and titanium

526   phosphate (TiP) under solar radiation. *Journal of Molecular Catalysis A: Chemical,*

527   *261*, 241-261.

528   Forgacs, E., Cserháti, T., & Oros, G. (2004). Removal of synthetic dyes from wastewaters: a

529   review. *Environmental International, 30*, 953-971.

530 Franco, A., Neves, M. C., Carrott, M. M. L., Mendonca, M. H., Pereira, M. I., & Monteiro, O.

531   C. (2009). Photocatalytic decolorization of Methylene Blue in the presence of

532   TiO_2/ZnS nanocomposites. *Journal of Hazardous Materials, 161*, 545-550.

533 Fu, Z., Zhang, Y., & Wang, X. (2011). Textile wastewater treatment using anoxic filter bed

534   and biological wriggle bed-ozone biological aerated filter. *Bioresource Technology,*

535   *102*, 3748-3753.

536 Gaca, J., Kowalska, M., & Mróz, M. (2005). The effect of chloride ions on

537   alkylbenzenesulfonate degradation in the Fenton reagent. *Polish Journal of*

538   *Environmental Studies, 14*, 23-27.

539 Ghaly, M. Y., Farah, J. Y., & Fathy, A. M. (2007). Enhancement of decolorization rate and

540   COD removal from dyes containing wastewater by the addition of hydrogen peroxide

541   under solar photocatalytic oxidation. *Desalination, 217*, 74-84.

542 Ghaly, M. Y., Jamil, T. S., El-Seesy, I. E., Souaya. E. R., & Nasr, R.A. (2011). Treatment of

543   highly polluted paper mill wastewater by solar photocatalytic oxidation with

544   synthesized nano TiO_2. *Chemical Engineering Journal, 168*, 446-454.

545 Giri, R. R., Ozaki, H., Takayanagi, Y., Taniguchi, S., & Takanami, R. (2011). Efficacy of

546   ultraviolet radiation and hydrogen peroxide oxidation to eliminate large number of

547   pharmaceutical compounds in mixed solution. *International Journal of Environmental*

548   *Science and Technology, 8*, 19-30.

549   Güçlü, D., Şirin, N., Şahinkaya, S., & Sevimli, M. F. (2013). Advanced treatment of coking

550   wastewater by conventional and modified Fenton processes. *Environmental Progress*

551   *and Sustainable Energy, 32*, 176-180.

552   Gümüş, D., & Akbal, F. (2011). Photocatalytic degradation of textile dye and wastewater.

553   *Water, Air, & Soil Pollution, 216*, 117-124.

554   Hashim, H. A. A., Mohamed, A. R., & Lee, K. T. (2001). Solar photocatalytic degradation of

555   Tartrazine using titanium oxide. *Jurnal Teknologi, 35*, 31-40.

556   Herney-Ramirez, J., Vicente, M. A., & Madeira, L. M. (2010). Heterogeneous photo-Fenton

557   oxidation with pillard clay-based catalysts for wastewater treatment: a review. *Applied*

558   *Catalysis B: Environmental, 98*, 10-26.

559   Houas, A., Lachheb, H., Ksibi, M., Elaloui, E., Guillard, C., & Hermann, J. M. (2001).

560   Photocatalytic degradation pathway of Methylene Blue in water. *Applied Catalysis B:*

561   *Environmental, 31*, 145-157.

562   Kansal, S. K., Singh, M., & Sud, D. (2007). Studies on photodegradation of two commercial

563   dyes in aqueous phase using different photocatalysts. *Journal of Hazardous Materials,*

564   *141*, 581-590.

565   Kavitha, S. K., & Palanisamy, P. N. (2010). Solar photocatalytic degradation of Vat Yellow 4

566   dye in aqueous suspension of TiO_2 - optimization of operational parameters.

567   *International Journal of Bioflux Society, 2*, 189-202.

568   Kitture, R., Koppikar, S. J., Kaul-Ghanekar, R., & Kale, S. N. (2010). Catalyst efficiency,

569   photostability and reusability study of ZnO nanoparticles in visible light for dye

570   degradation. *Journal of Physics and Chemistry of Solids, 72*, 60-66.

571   Kumar, J., & Bansal, A. (2012). Photodegradation of Amaranth in aqueous solution catalyzed

572   by immobilized nanoparticles of titanium oxide. *International Journal of*

573   *Environmental Science and Technology, 9*, 479-484.

574   Kumar, J., & Bansal, A. (2013). A comparative study of immobilization techniques for

575   photocatalytic degradation of Rhodamine B using nanoparticles of titanium dioxide.

576   *Water, Air, & Soil Pollution, 224*, 1-11.

577   Lachheb, H., Puzenat, E., Houas, A., Elalaoui, E., Guilard, C., Hermann, J. M., & Mohamed,

578   K. (2002). Photocatalytic degradation of various types of dyes (Alizarin S,Crocein

579   Orange G, Methyl Red, Congo Red, Methylene Blue) in water by UV-irradiated

580   titania. *Applied Catalysis B: Environmental, 39*, 75-90.

581   Lee, B. N., Liaw, W. D., & Lou, J. C. (1999). Photocatalytic decolorization of Methylene Blue

582   in aqueous TiO_2 suspension. *Environmental Engineering Science, 16*, 165-175.

583   Lee, E., Lee, H., Kim, Y. K., Sohn, K., & Lee, K. (2011). Hydrogen peroxide interference in

584   chemical oxygen demand during ozone based advanced oxidation of anaerobiacally

585   digested livestock wastewater. *International Journal of Environmental Science and*

586   *Technology, 8*, 381-388.

587   Li, F. B., & Li, X. Z. (2002). The enhancement of photodegradation efficiency using $Pt-TiO_2$

588   catalyst. *Chemosphere, 48*, 1103-1111.

589   Lin, X., Huang, F., Wang, W., & Shi, J. (2007). Photocatalytic activity of $Bi_{24}Ga_2O_{39}$ for

590   degrading Methylene Blue. *Scripta Materialia, 56*, 189-192.

591 Lodha, S., Jain, A., & Punjabi, P. B. (2010). A comparative study of photocatalytic

592   degradation of Methylene Blue in presence of some transition metal complexes and

593   hydrogen peroxide. *Malaysian Journal of Chemistry, 120*, 19-26.

594 Lotito, A. M., Fratino, U., Bergna, G., & Iaconi, C. D. (2012). Integrated biological and ozone

595   treatment of printing textile wastewater. *Chemical Engineering Journal, 195-196*, 261-

596   269.

597 Low, F. C. F., Wu, T. Y., Teh, C. Y., Juan, J. C., & Balasubramaniam, N. (2012).

598   Investigation into photocatalytic decolorisation of CI Reactive Black 5 using titanium

599   dioxide nanopowder. *Coloration Technology, 128*, 44-50.

600 Mohapatra, P., & Parida, K. M. (2006). Photocatalytic activity of sulfate modified titania 3:

601   decolorization of Methylene Blue in aqueous solution. *Journal of Molecular Catalysis*

602   *A: Chemical, 258*, 118-123.

603 Mota, A. L. N., Albuquerque, L. F., Beltrame, L. T. C., Chiavone-Filho, O., Machulek, Jr. A,

604   & Nascimento, C. A. O. (2008). Advanced oxidation process and their application in

605   the petroleum industry: a review. *Brazilian Journal of Petroleum and Gas, 2*, 122-142.

606 Muruganandham, M., Sobana, N., & Swaminathan, M. (2007). Solar assisted photocatalytic

607   and photochemical degradation of Reactive Black 5. *Journal of Hazardous Materials*

608   *B, 137*, 1371-1376.

609   National Toxicology Program, 2013. Executive summary of safety and toxicity information:

610   Methylene Blue. http://ntp.niehs.nih.gov/?objectid=03DB4384-0364-AB0B-

611   5C71EF4A37D6888A#NOM. Accessed 16 October 2013.

612   Neppolian, B., Choi, H. C., Sakthivel, S., Arabindoo, B., & Murugesan, V. (2002). Solar light

613   induced and TiO_2 assisted degradation of textile dye Reactive Blue 4. *Chemosphere,*

614   *46*, 1173-1181.

615   Nezamzadeh-Ejhieh, A., & Hushmandrad, S. (2010). Solar photodecolorization of Methylene

616   Blue by CuO/X zeolite as a heterogeneous catalyst. *Applied Catalysis, 338*, 149-159.

617   Nouri, J., Nouri, N., & Moeeni, M. (2012). Development of industrial waste disposal scenarios

618   using life-cycle assessment approach. *International Journal of Environmental Science*

619   *and Technology, 9*, 417-424.

620   Ong, S.-A., Min, O.-M., Ho, L.-N., & Wong, Y.-S. (2012). Comparative study on

621   photocatalytic degradation of mono azo dye acid orange 7 and methyl orange under

622   solar light irradiation. *Water, Air, & Soil Pollution, 223*, 5483-5493.

623   Pang, Y. L., & Abdullah, A. Z. (2013). Current status of textile industry wastewater

624   management and research progress in Malaysia: A review. *Clean – Soil, Air, Water,*

625   *41*, 751-764.

626   Pardeshi, S. K., & Patil, A. B. (2009). Solar photocatalytic degradation of resorcinol a model

627   endocrine disrupter in water using zinc oxide. *Journal of Hazardous Materials, 163*,

628   403-409.

629   Poulios, I., & Aetopoulou, I. (1999). Photocatalytic degradation of the textile dye Reactive

630   Orange 16 in the presence of TiO_2 suspensions. *Environmental Technology, 20*, 479-

631   487.

632 Pouretedal, H. R., & Kadkhodaie, A. (2010). Synthetic CeO_2 nanoparticle catalysis of

633   methylene blue photodegradation: kinetics and mechanism. *Chinese Journal of*

634   *Catalysis, 31*, 1328-1334.

635 Saheed, H. (2012). Prospects for the textile and clothing industry in Malaysia. *Textile Outlook*

636   *International, 158*, 64-101.

637 Saif Ur Rehman, M., & Han, J. I. (2013). Biosorption of methylene blue from aqueous

638   solutions by *Typha angustata* phytomass. *International Journal of Environmental*

639   *Science and Technology, 10*, 865-870.

640 Senthilkumaar, S., Porkodi, K., Gomathi, R., Maheswari, A. G., & Manomani, N. (2006). Sol

641   gel derived silver doped nanocrystalline titania catalysed photodegradation of

642   Methylene Blue from aqueous solution. *Dyes and Pigments, 69*, 22-30.

643 Sievers, M. (2011). Advanced oxidation processes. *Treatise on Water Science, 4*, 377-408.

644 Song, Y., & Bai, B. (2010). TiO_2-assisted photodegradation of Direct Blue 78 in aqueous

645   solution in sunlight. *Water, Air, & Soil Pollution, 213*, 311-317.

646 Su, T.-L., Kuo, Y.-L., Wu, T.-J., & Kung, F.-C. (2012). Experimental analysis and

647   optimization of the synthesizing property of nitrogen-modified TiO_2 visible-light

648   photocatalysts. *Journal of Chemical Technology and Biotechnology, 87*, 160-164.

649 Sun, D., Zhang, X., Wu, Y., & Liu, T. (2013). Kinetic mechanism of competitive adsorption

650   of disperse dye and anionic dye on fly ash. *International Journal of Environmental*

651   *Science and Technology, 10*, 799-808.

652   Tabaei, H. S. M., Kazemeini, M., & Fattahi, M. (2012). Preparation and characterization of

653   visible light sensitive nano titanium dioxide photocatalyst. *Scientia Iranica C, 19*,

654   1626-1631.

655   Vujevic, D., Papic, S., Koprivanac, N., & Bozic, A. (2010). A decolorization and

656   mineralization of reactive dye by UV/Fenton process. *Separation Science and*

657   *Technology, 45*, 637–1643.

658   Wang, K. H., Hsieh, Y. H., Wu, C. H., & Cheng, C. Y. (2000). The pH and anion effects on

659   the heterogeneous photocatalytic degradation of o-methylebenzoic acid in TiO_2

660   aqueous suspension. *Chemosphere, 40*, 389-394.

661   Wang, S., Li, D., Sun, C., Yang, S., Guan, Y., & He, H. (2014). Highly efficient photocatalytic

662   treatment of dye wastewater via visible-light-driven $AgBr-Ag_3PO_4$ / MWCNTs.

663   *Journal of Molecular Catalysis A: Chemical, 383-384*, 128-136.

664   Wu, C. H., & Chern, J. M. (2006). Kinetics of photocatalytic decomposition of Methylene

665   Blue. *Industrial and Engineering Chemistry Research, 45*, 6450-6457.

666   Wu, T. Y., Guo, N., Teh, C. Y., & Hay, J. X. W. (2013). Advances in Ultrasound Technology

667   for Environmental Remediation. *SpringerBriefs in Molecular Science*, doi:

668   10.1007/978-94-007-5533-8

669   Xiao, Q., Zhang, J., Xiao, C., Si, Z., & Tan, X. (2008). Solar photocatalytic degradation of

670   Methylene Blue in carbon-doped TiO_2 nanoparticles suspension. *Solar Energy, 82*,

671   706-713.

672   Yang, Y., Wu, Q., Guo, Y., Hu, C., & Wang, E. (2005). Efficient degradation of dye

673   pollutants on nanoporous polyoxotungstate-anatase composite under visible-light

674   irradiation. *Journal of Molecular Catalysis A: Chemical, 225*, 203-212.

675   Zhou, B., Zhao, X., Liu, H., Qu, J., & Huang, C. P. (2010). Visible-light Sensitive cobalt-

676   doped $BiVO_4$ (Co-$BiVO_4$) photocatalytic composites for the degradation of Methylene

677   Blue dye in dilute aqueous solutions. *Applied Catalysis B-Environmental, 99*, 214-221.

678
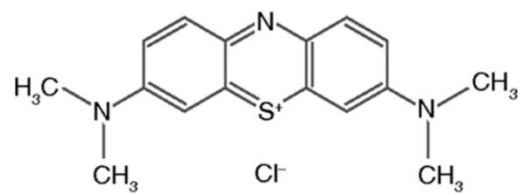
Fig. 1 Molecular structure of methylene blue
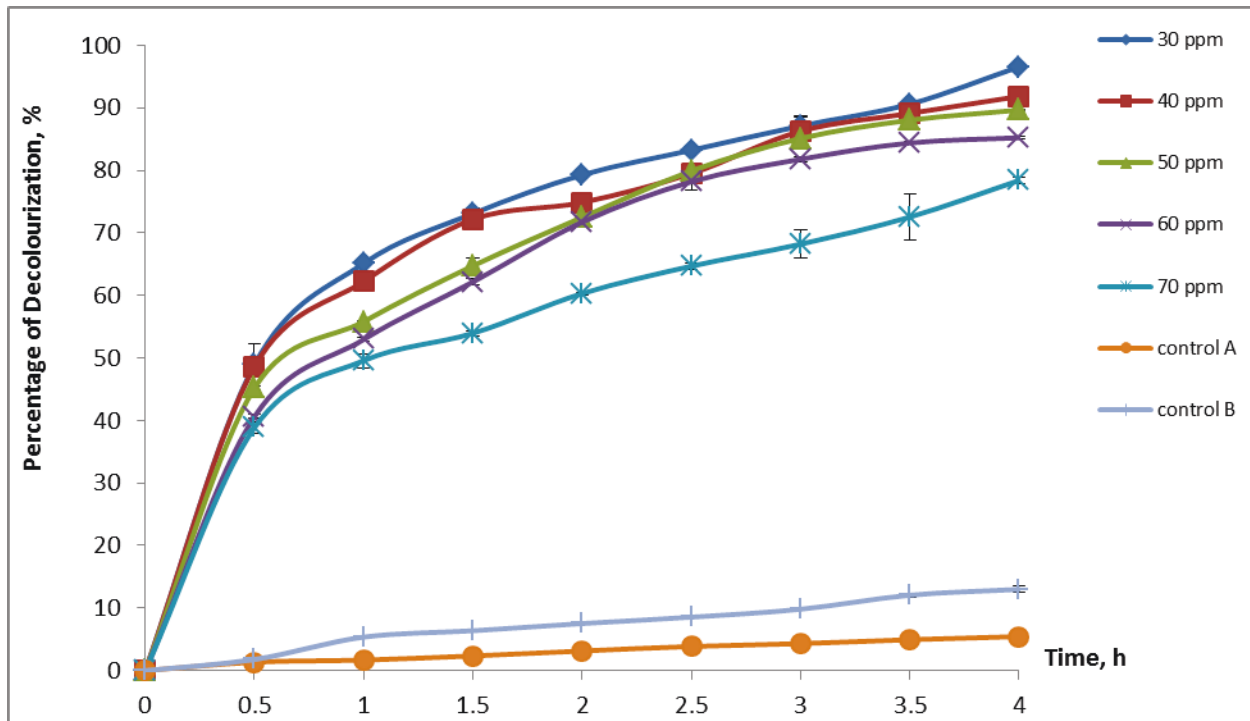
Fig. 2 (a) Effect of initial concentration on the decolourization efficiency of MB; (b) Plot of ln C against time for different initial concentration of MB. The results are averages of triplicate tests. Fixed operating parameters: $[TiO_2]$ = 1.0 g/L; pH = 10.5
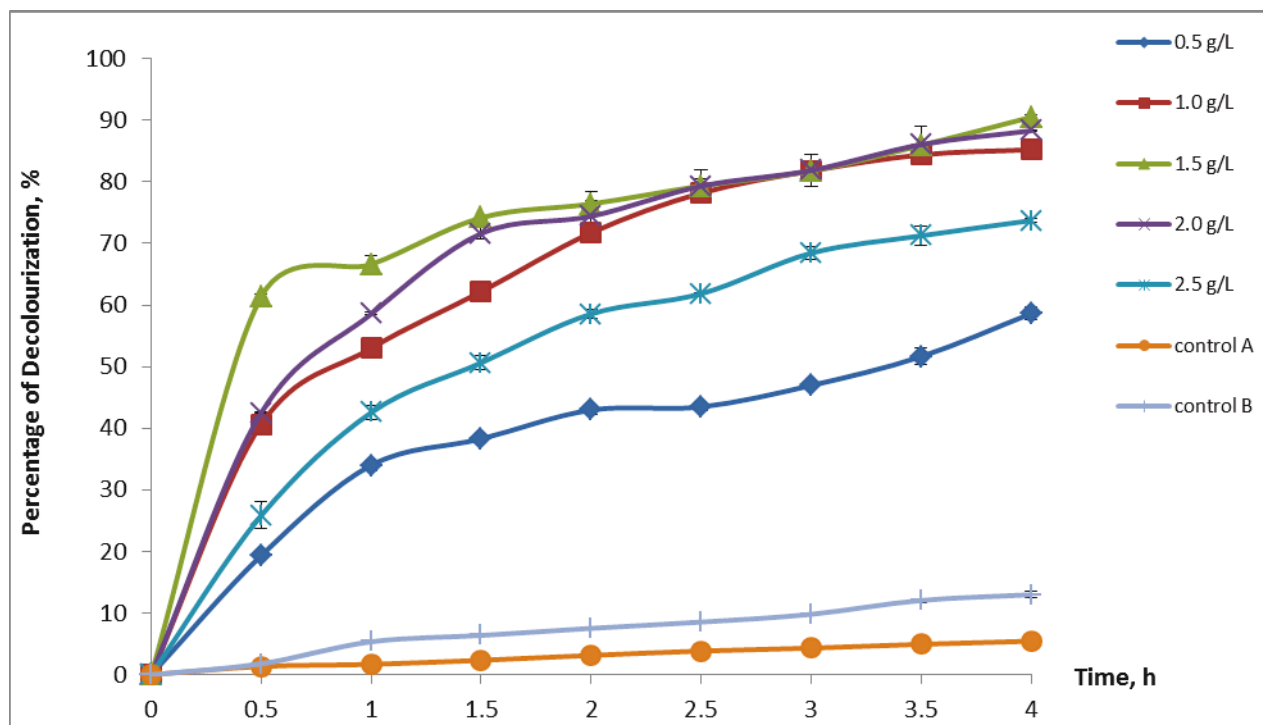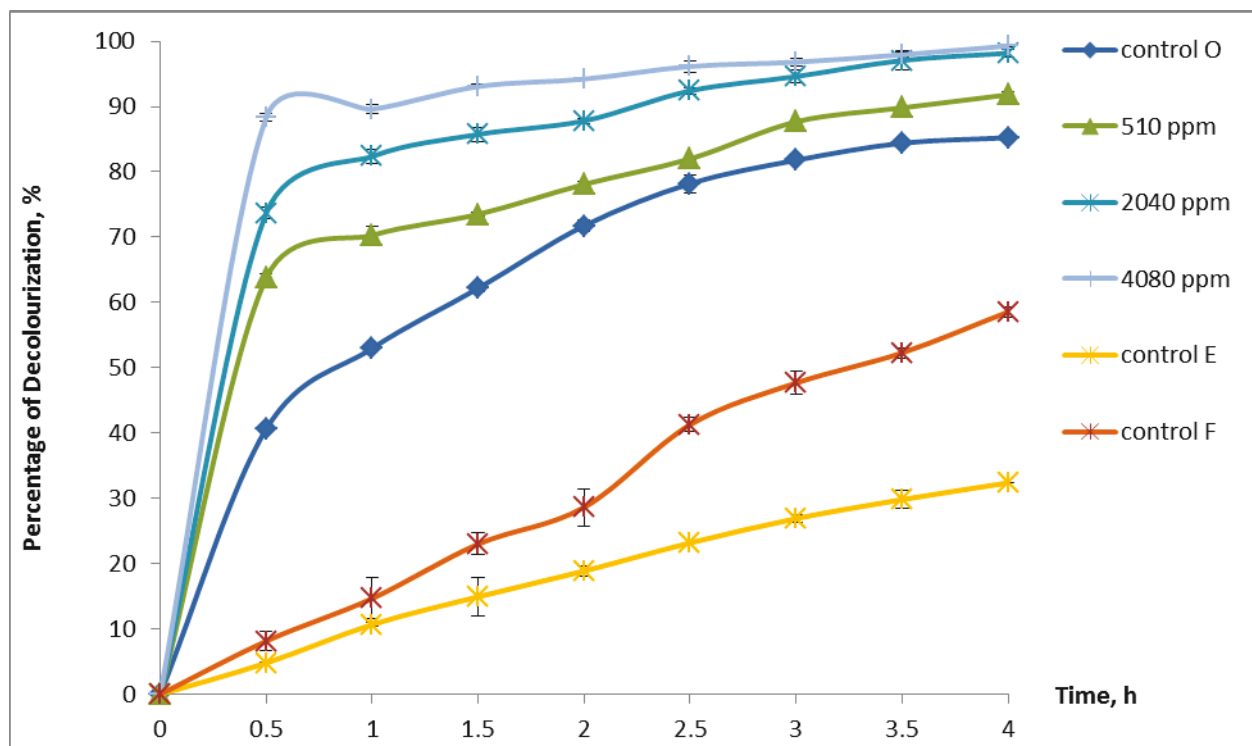
Fig. 3 (a) Effect of catalyst loading on the decolourization efficiency of MB; (b) Plot of ln C against time for different catalyst loading. The results are averages of triplicate tests. Fixed operating parameters: [MB] = 60 ppm; pH = 10.5
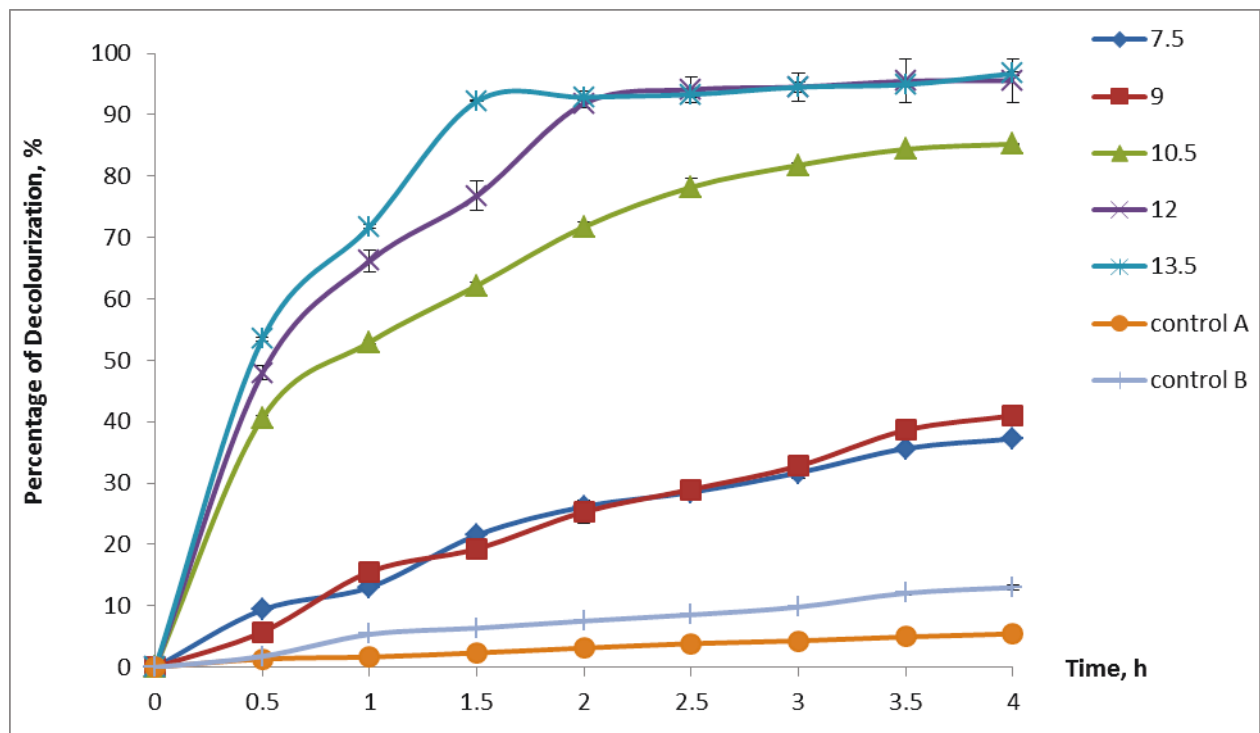
Fig. 4 (a) Effect of initial pH on the decolourization efficiency of MB; (b) Plot of ln C against time for different pH values. The results are averages of triplicate tests. Fixed operating parameters: [MB] = 60 ppm; [TiO_2] = 1.0 g/L
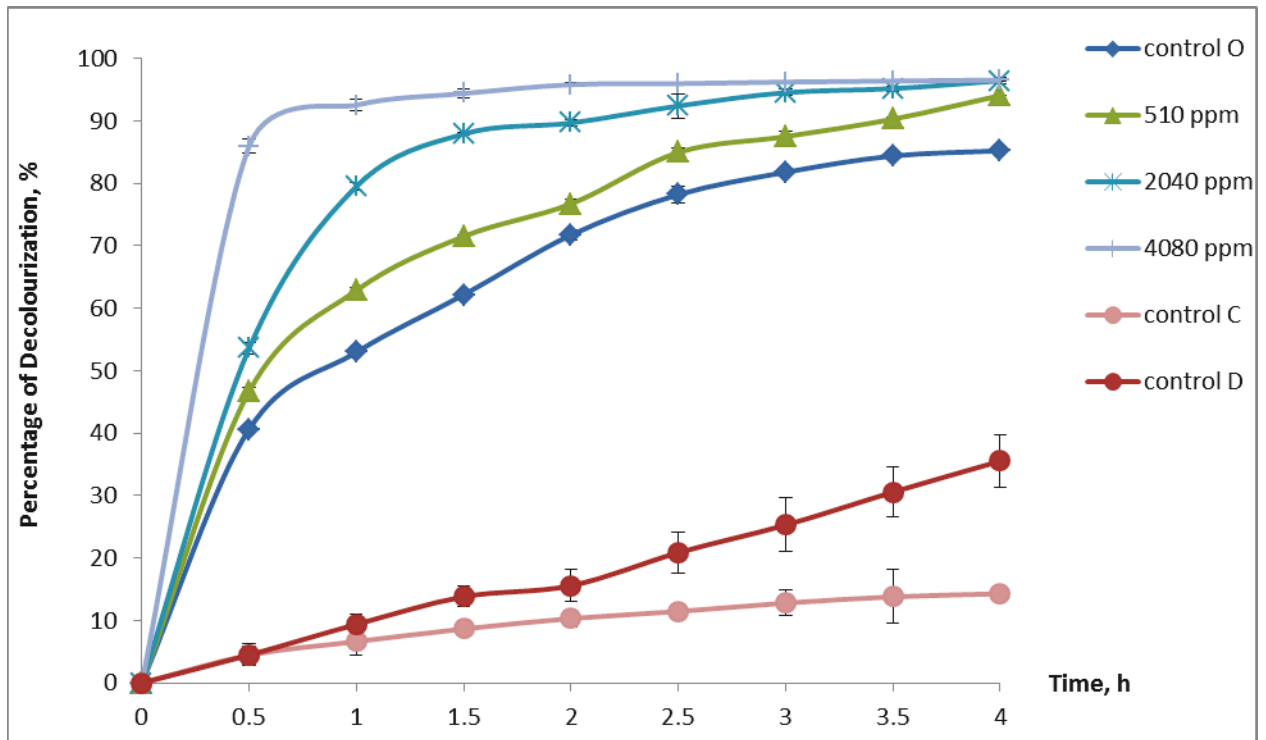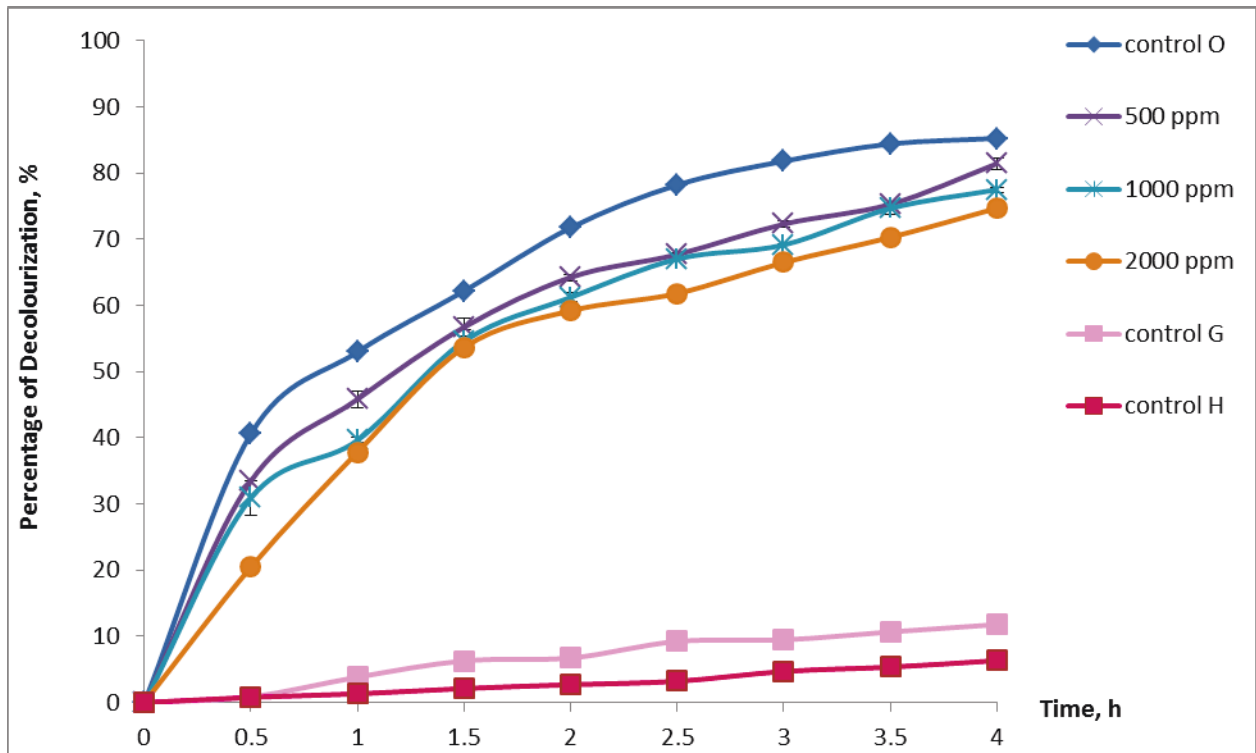
Fig. 5 (a) Effect of H_2O_2 on the decolourization efficiency of MB; (b) Plot of ln C against time for different concentration of H_2O_2. The results are averages of triplicate tests. Fixed operating parameters: [MB] = 60 ppm; [TiO_2] = 1.0 g/L; pH = 10.5
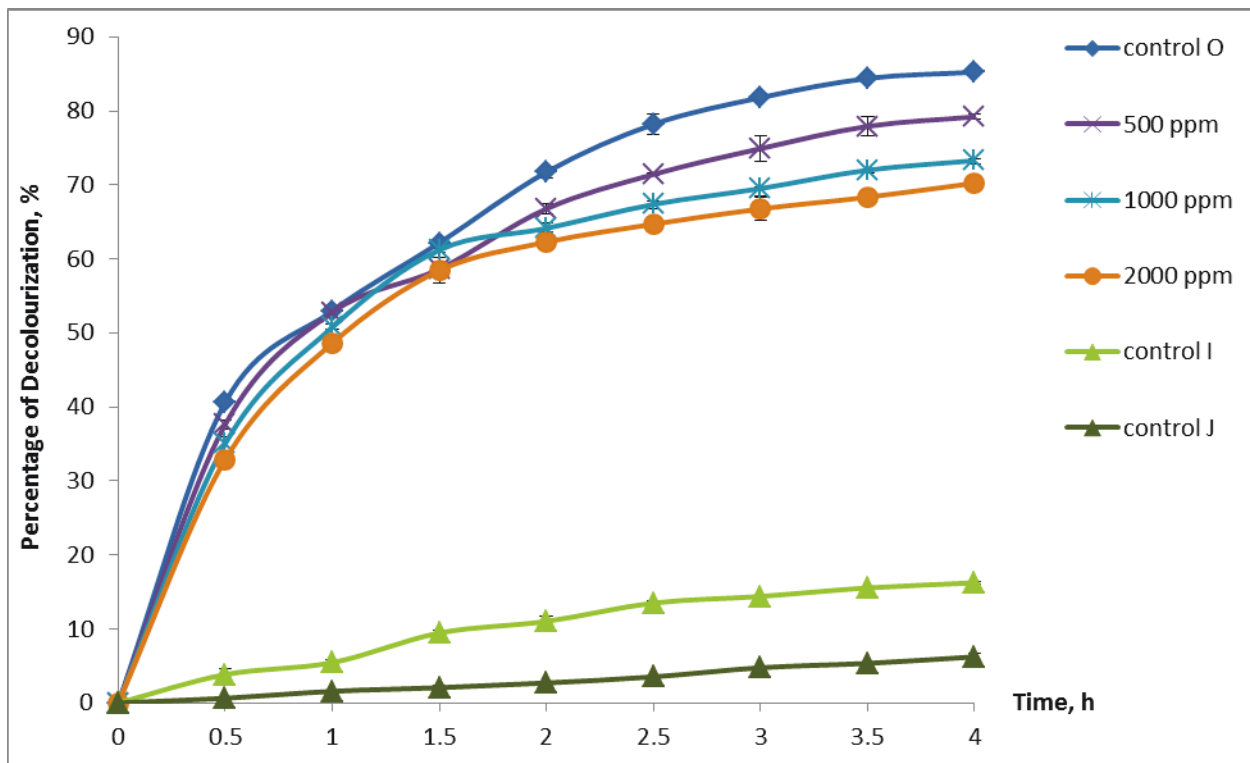
Fig. 6 (a) Effect of $S_2O_8^{2-}$ on the decolourization efficiency of MB; (b) Plot of ln C against time for different concentration of $S_2O_8^{2-}$. The results are averages of triplicate tests. Fixed operating parameters: [MB] = 60 ppm; [TiO$_2$] = 1.0 g/L; pH = 10.5

Fig. 7 (a) Effect of Cl⁻ on the decolourization efficiency of MB; (b) Plot of ln C against time for different concentration of Cl⁻. The results are averages of triplicate tests. Fixed operating parameters: [MB] = 60 ppm; [TiO$_2$] = 1.0 g/L; pH = 10.5

Fig. 8 (a) Effect of CO_3^{2-} on the decolourization efficiency of MB; (b) Plot of ln C against time for different concentration of CO_3^{2-}. The results are averages of triplicate tests. Fixed operating parameters: [MB] = 60 ppm; [TiO_2] = 1.0 g/L; pH = 10.5

Table 1 Experimental operating parameters of each control experimental run

Control	Operating parameters at [MB] = 60 ppm and pH = 10.5
A	Catalysis
B	Photolysis
C	Catalysis; $[H_2O_2]$ = 4080 ppm
D	Photolysis; $[H_2O_2]$ = 4080 ppm
E	Catalysis; $[S_2O_8^{2-}]$ = 4080 ppm
F	Photolysis; $[S_2O_8^{2-}]$ = 4080 ppm
G	Catalysis; $[Cl^-]$ = 2000 ppm
H	Photolysis; $[Cl^-]$ = 2000 ppm
I	Catalysis; $[CO_3^{2-}]$ = 2000 ppm
J	Photolysis; $[CO_3^{2-}]$ = 2000 ppm
O	Photo-catalysis using 1 g/L of TiO_2 without incorporating additives

Catalysis = Experiment conducted in the dark with 1.0 g/L of TiO_2

Photolysis = Experiment conducted under sunlight without any catalyst

Table 2 Pseudo-first-order rate constants, k_{app} for different initial concentration of MB, catalyst loading and initial pH values

Initial concentration of MB, ppm	$10^3 k_{app}$, min^{-1}	Correlation coefficient, R^2
30	18.1	0.976
40	16.1	0.948
50	13.2	0.983
60	10.8	0.945
70	8.23	0.888
Catalyst loading, g/L	$10^3 k_{app}$, min^{-1}	Correlation coefficient, R^2
0.5	4.54	0.767
1.0	10.8	0.945
1.5	12.6	0.817
2.0	11.7	0.936
2.5	7.99	0.892
Initial pH	$10^3 k_{app}$, min^{-1}	Correlation coefficient, R^2
7.5	2.97	0.704
9.0	2.87	0.929
10.5	10.8	0.945
12.0	19.5	0.979
13.5	25.9	0.973

Table 3 Comparison of pseudo-first-order rate constants, k_{app} between different additives

Initial concentration of additive, ppm		$10^3 k_{app}$, min^{-1}	Correlation coefficient, R^2
No additives (control O)		10.8	0.945
H_2O_2	510	14.9	0.973
	2040	26.3	0.965
	4080	66.2	0.988
$S_2O_8^{2-}$	510	14.7	0.890
	2040	56.8	0.969
	4080	91.0	0.999
Cl^-	500	9.2	0.890
	1000	8.4	0.896
	2000	7.8	0.885
CO_3^{2-}	500	9.4	0.885
	1000	8.2	0.876
	2000	7.3	0.845

Experimental conditions: [MB]= 60 ppm, [TiO$_2$]= 1.0 g/L, pH= 10.5

Table 4 Comparison of pseudo-first-order rate constants, k_{app} for decolourization of MB using TiO_2 between present and previous studies

Initial Concentration of MB, ppm	$10^3 k_{app}$, min^{-1}	Experimental Conditions	Reference
60 (without any additive) 60 (with 4080 ppm $S_2O_8^{2-}$)	10.8 91.0	$[TiO_2]$= 1.0 g/L Initial pH=10.5 Irradiation= sunlight Irradiation time= 240 min	Present study
27	53.0	$[TiO_2]$= 0.5 g/L pH= 7 Irradiation= UV light Irradiation time= 200 min	Lachheb et al., 2002
3	67	$[TiO_2]$= 0.25 g/L Initial pH= 3 Irradiation= UV light Irradiation time= 60 min	Lee et al., 1999
23	60	$[TiO_2]$= 2.5 g/L pH= 6 Irradiation= UV light Irradiation time= 90 min	Houas et al., 2001
10	29.3	$[TiO_2]$= 2.0 g/L Initial pH= unspecified Irradiation= visible light Irradiation time= 600 min	Lin et al., 2007
6	45.4	$[TiO_2]$= 0.7 g/L Initial pH=4.3 Irradiation= UV light Irradiation time= 80 min	Chen et al., 2003
15	67.2	$[TiO_2]$= 1.2 g/L Initial pH= unspecified Irradiation= UV light Irradiation time= 30 min	Li and Li, 2002